

Identification of Deep Brain Stimulation Targets for Neuropathic Pain After Spinal Cord Injury Using Localized Increases in White Matter Fiber Cross-Section

Shana R. Black, MS^{1,2} ; Andrew Janson, PhD³; Mark Mahan, MD⁴; Jeffrey Anderson, MD, PhD^{1,5}; Christopher R. Butson, PhD^{1,2,4,6,7}

ABSTRACT

Objectives: The spinal cord injury (SCI) patient population is overwhelmingly affected by neuropathic pain (NP), a secondary condition for which therapeutic options are limited and have a low degree of efficacy. The objective of this study was to identify novel deep brain stimulation (DBS) targets that may theoretically benefit those with NP in the SCI patient population. We hypothesize that localized changes in white matter identified in SCI subjects with NP compared to those without NP could be used to develop an evidence-based approach to DBS target identification.

Materials and Methods: To classify localized neurostructural changes associated with NP in the SCI population, we compared white matter fiber density (FD) and cross-section (FC) between SCI subjects with NP ($N = 17$) and SCI subjects without NP ($N = 15$) using diffusion-weighted magnetic resonance imaging (MRI). We then identified theoretical target locations for DBS using fiber bundles connected to significantly altered regions of white matter. Finally, we used computational models of DBS to determine if our theoretical target locations could be used to feasibly activate our fiber bundles of interest.

Results: We identified significant increases in FC in the splenium of the corpus callosum in pain subjects when compared to controls. We then isolated five fiber bundles that were directly connected to the affected region of white matter. Our models were able to predict that our fiber bundles of interest can be feasibly activated with DBS at reasonable stimulation amplitudes and with clinically relevant implantation approaches.

Conclusions: Altogether, we identified neuroarchitectural changes associated with NP in the SCI cohort and implemented a novel, evidence-driven target selection approach for DBS to guide future research in neuromodulation treatment of NP after SCI.

Keywords: Deep brain stimulation, diffusion weighted MRI, fiber-specific white matter, neuropathic pain, spinal cord injury

Conflict of Interest: Christopher R. Butson, PhD, has served as a consultant for NeuroPace, Advanced Bionics, Boston Scientific, Intelect Medical, Abbott, NeuraModix, and Functional Neuromodulation. The remaining authors have no conflicts to disclose.

INTRODUCTION

Neuropathic pain (NP) is formally classified as pain caused by a primary lesion or dysfunction of the somatosensory system (1). Of the estimated 294,000 people in the United States currently living with chronic spinal cord injury (SCI) (2), approximately 80% are reported to be affected by this debilitating condition (3). Despite this high prevalence, scientific understanding of the neurological mechanisms of NP in the SCI population is not well understood and effective treatment approaches remain elusive. Previous studies have shown that sensorimotor and emotional processing regions of the brain, including cingulate, prefrontal cortex, thalamus, and insula, are associated with the perception and persistence of symptoms in other NP populations; and that the patterns of neurological change are specific to the primary diagnosis that results in NP (4–9). Further, neurostructural changes in the limbic system have been hypothesized to be particularly promising in the identification of population-specific biomarkers (10). The expression and perception of pain is known to be, in part, driven

Address correspondence to: Christopher R. Butson, PhD, Warnock Engineering Building, 72 South Central Campus Drive, Room 3686, Salt Lake City, UT 84112, USA. Email: butson@sci.utah.edu

¹ Biomedical Engineering, University of Utah, Salt Lake City, UT, USA;

² Scientific Computing and Imaging Institute, University of Utah, Salt Lake City, UT, USA;

³ Vanderbilt University Institute of Imaging Science, Department of Radiology and Radiological Sciences, Vanderbilt University Medical Center, Nashville, TN, USA;

⁴ Neurosurgery, University of Utah, Salt Lake City, UT, USA;

⁵ Radiology and Imaging Sciences, University of Utah, Salt Lake City, UT, USA;

⁶ Neurology, University of Utah, Salt Lake City, UT, USA; and

⁷ Psychiatry, University of Utah, Salt Lake City, UT, USA

For more information on author guidelines, an explanation of our peer review process, and conflict of interest informed consent policies, please go to <http://www.wiley.com/WileyCDA/Section/id-301854.html>

Source(s) of financial support: Funding for this study was provided by the University of Utah Neuroscience Initiative. Shana R. Black is supported by the NSF Graduate Research Fellowship Program (1747505). Shana R. Black, Andrew Janson, and Christopher R. Butson are supported by NIH UH3NS095554.

by emotional responses specifically within the limbic system (11,12). Changes within limbic circuitry as they relate to specific pain causes and qualities have been further hypothesized to be key to the identification of targets for therapeutic intervention to improve the outcomes of patients with NP (10).

Currently, less than 35% of NP patients receive notable benefit from first-line therapies (13). NP is also known to be resistant to opioids and anti-inflammatory pharmacological treatments (13), which further highlights the need for the development of novel treatment strategies. Deep brain stimulation (DBS) is a neuromodulation therapy that has been used to effectively treat a range of movement disorders and psychiatric conditions (14). The potential for DBS therapy to improve outcomes for patients with other neurological conditions is promising, but is limited by the identification of condition-specific stimulation targets (14). DBS has been used in the past to improve chronic NP symptoms, suggesting that it may be a viable option for treatment (15,16). However, results have been mixed in those with central NP (16), warranting additional research into condition-specific targeting approaches. Previous attempts to treat NP after SCI using DBS have been largely unsuccessful (17). However, the targeting approach for these prior studies has been limited to a very small number of targets based on traditional pain related circuitry (17,18), further highlighting the need for additional research and new, evidence-based, and population-specific approaches to identifying DBS targets for the treatment of NP.

Localized changes in white matter have been shown to be specifically indicative of alterations in pain perception and the chronicification of pain in other patient populations (19–21). Identifying and targeting population-specific microstructural changes in white matter may therefore be beneficial in the treatment of NP and improve patient outcomes. In this study, we implement a novel and robust method using magnetic resonance imaging (MRI) to identify localized, fiber-specific changes in white matter structure associated with NP in subjects with SCI compared to SCI subjects without NP symptoms. We then use tractography and white matter connectivity to identify potential DBS targets based on the spatial distribution of changes in white matter associated with NP. Finally, we assess the feasibility of DBS at each of these target locations using computational models. By using this evidence-driven approach to DBS target selection, we can better inform the development of clinical research and therapeutic methods and increase our understanding of the neuroarchitectural correlates of NP in the SCI. Through the examination of the theoretical activation patterns resultant of stimulation at these target locations, we provide insight for future DBS research that could better treat NP symptoms in patients with SCI.

MATERIALS AND METHODS

Subject Selection

We selected subjects via medical record review based on the following inclusion and exclusion criteria: 1) individuals must have sustained a traumatic SCI at least one year prior to enrollment; 2) individuals must be between 18 and 45 years of age at the time of enrollment; 3) medical records must show that individuals have an American Spinal Cord Injury Association Impairment Scale (AIS) classification of either A or B, indicating that they do not have motor function below their level of SCI; 4) individuals cannot have any medical history of diabetes, cancer, amputation, brain injury, stroke, or any neurological injury or condition other than SCI; 5)

individuals do not report any pain condition, such as arthritis, other than NP; 6) individuals do not have any conditions with which an MRI would be unsafe. The cohort in this study is a subset of those reported in prior publications (S.R. Black et al., unpublished data). For this work, we included subjects for whom the diffusion weighted imaging (DWI) was of sufficient quality for fiber specific white matter analysis.

We collected demographic information, a verified medical history, and a series of patient reported outcomes from all participants. Outcomes included maximum subscores from the Neuropathic Pain Symptom Inventory (NPSI) (22), severity and interference scores from the Brief Pain Inventory (BPI) (23), and anxiety and depression scores from the Hospital Anxiety and Depression Scale (HADS) (24). All subjects also provided a pain rating on an 11 point (0–10) numeric pain rating scale (NPRS) at the time they underwent MRI study procedures. Responses to the pain rating scales—NPSI, BPI, and NPRS—determined whether subjects were categorized as part of the pain group or control group.

There were 32 subjects (25 male) included in this study. Seventeen (12 male) were categorized into the pain group and 15 (13 male) lacked pain symptoms and were categorized into the control group. We used independent *t*-tests to compare groupwise demographic information, and anxiety, depression, and pain outcomes. Table 1 shows the demographic and SCI information as well as the average pain, anxiety, and depression outcome scores for the pain and control groups. All subjects provided informed consent to undergo study procedures and the full study protocol was approved of by the University of Utah Institutional Review Board.

Image Acquisition and Analysis

All subjects in this study underwent imaging procedures in the same Siemens PRISMA 3T system in the Utah Center for Advanced Imaging Research (UCAIR) at the University of Utah. We used a 64-channel head coil to obtain structural MRI and DWI. T1 weighted structural imaging was obtained using an MP2RAGE sequence with isotropic 1 mm voxel resolution, 5000 ms

Table 1. Groupwise Summary of Demographics, SCI Statistics, and Depression, Anxiety, and Pain Metrics.

Variable	Pain group	Control group
Sex (M/F)	12/5	12/3
Mean age (SD)	31.24 (8.76)	28.60 (5.98)
Tetraplegic	9	11
Paraplegic	8	4
Time since SCI in months (SD)	101.12 (88.42)	89.4 (62.08)
Method of injury		
Vehicular	10	9
Fall	1	1
Sports	6	4
Other	0	1
Mean HADS Depression score (SD)*	4.18 (2.87)	1.93 (1.69)
Mean HADS Anxiety score (SD)†	6.12 (3.16)	1.93 (1.48)
Mean NPSI maximum subscore (SD)	5.26 (1.78)	-
Mean NPRS at scan time (SD)	3.18 (1.60)	-
Mean BPI Severity score (SD)	3.64 (1.78)	-
Mean BPI Interference score (SD)	2.88 (2.33)	-

*Significant difference between groups ($p < 0.05$).

†Significant difference between groups ($p < 0.0001$).

repetition time (TR), and 2.93 ms time to echo (TE). Multiband multishell DWI was obtained with isotropic 1.5 mm resolution, 187 diffusion directions, 4870 ms TR, 92.4 ms TE, a multiband acceleration factor of three, a flip angle of 78 degrees, and a maximum b -value of 3000 s/mm² (2). We also acquired a baseline scan with reverse polarity of the phase-encoding direction for each subject to assist in distortion correction during image preprocessing.

Initial preprocessing of DWI data sets included motion, distortion, and eddy current correction, which was done using the Functional Magnetic Resonance Imaging of the Brain Software Library (FSL) (25–28). We used MRtrix3 (29) for bias field corrections, intensity normalization, and all other analysis steps. After preprocessing, we performed a fixel-based analysis of fiber density (FD) and cross-section (FC). A fixel is defined as a specific fiber population within a voxel (30) and fixel-based analyses allow for identification, segmentation, and analysis of white matter with multiple fiber directions within each voxel.

In order to compute the spatial distribution of fibers within our cohort, we used a robust and fully automated method, developed by Dhollander et al. (31), to obtain response functions representing single-fiber white matter, gray matter, and cerebrospinal fluid from an average of all subjects from this study. We then used multishell, three-tissue, constrained spherical deconvolution to generate fiber orientation distribution (FOD) maps for each subject. These subject-specific FOD maps were then used to create a study-specific FOD template and fixel segmentation. Fixel segmentation is completed by sampling the orientation and amplitude of each lobe in the FOD map, segmenting fiber tracts relative to these lobes, and mapping the resultant streamlines to a voxel grid (32).

Subject-specific FOD maps were nonlinearly registered to the study-specific FOD template and fixel segmentation to assess group differences. We calculated the fixelwise FD for each subject directly from this registration by comparing the fiber bundle density of corresponding fixels from subject imaging to the population template. The FC is a relative metric indicating the cross-sectional size of each fixel relative to the study population. We calculated FC by measuring the magnitude of the warps required to register each fixel to the FOD template. In order to ensure that our data was normally distributed, we used the log of the FC metric for all subsequent analyses. We also computed a combined measure of fiber density and cross-section (FDC), which factors in the effects of both FD and FC.

Using the FOD template, we also generated a whole brain, spherical deconvolution informed filtered (SIFT) tractogram, which defines the pairwise connectivity between fixels to generate streamlines representing white matter fiber pathways within the brain (32). Using the tractogram template, we performed statistical analysis using connectivity-based fixel enhancement and nonparametric permutation testing to compare FD, FC, and FDC between groups with age, sex, and time since injury as nuisance covariates.

To better contextualize the results of the FD, FC, and FDC comparisons, we filtered the whole brain tractogram template to only include fiber tracts that pass through statistically significant fixels for each metric using a family-wise error (FWE) corrected alpha threshold of $p < 0.05$. We then separated the fibers passing through these fixels into distinct fiber bundles based on common convergent pathways and laterality. Finally, to identify cortical and subcortical endpoints of these fiber bundles, we converted each into a connectome using the Desikan-Killiany cortical parcellation (33) combined with a subcortical parcellation of gray matter nuclei to define the nodes. These connectomes were used to provide

qualitative insight into downstream regions of the brain that are directly connected to regions of significant, fiber-specific changes in white matter via pathways that are common to the cohort in this study.

DBS Targeting and Simulation

To assess the feasibility of using the significant changes in white matter that we had identified in our pain group subjects as a means for DBS target selection, we implemented a DBS modeling pipeline developed by Janson and Butson (34). We used SCIRun5 software (<https://sci.utah.edu/software/scirun.html>) to generate finite element models (FEMs) and simulate the effects of DBS on the fiber bundles that were isolated from our fiber specific white matter results. For a full description and details of our FEM and simulation parameters, see Supplementary Material Section 1, Supplementary Methods. Briefly, we generated a whole brain FEM mesh that consisted of the brain surface from the study-specific FOD template, each of the fiber bundles generated in “Image Acquisition and Analysis” section, and a model of a DBS electrode, which included the electrode contacts and shaft of the DBS lead. The DBS electrode model was manually placed for each simulation based on regions of convergent fibers within each of the bundles. We also consulted with a neurosurgeon specializing in DBS implantation in order to identify lead trajectories that would be clinically realistic. The voltage distribution across the brain was then calculated at each node in the mesh to determine whether fibers within each bundle were activated for a given simulation.

For each simulation, we either tried to stimulate a substantial proportion of one bundle individually or all of the bundles together within one hemisphere of the brain. The DBS electrodes were placed such that the most distal contact on the lead was central to the fiber bundle(s) and was used as the active contact for monopolar stimulation. For each simulated DBS target location, we calculated the voltage distribution for stimulation amplitudes ranging from -1 V to -5 V. Although the stimulator has the capability to apply up to -10 V, it is typically preferable to limit power consumption in order to preserve battery life. We therefore evaluated this lower range of amplitudes under the assumption that a well-placed lead will require lower amplitudes to achieve therapeutic effects and minimize activation of irrelevant brain structures. To predict the percentage of each fiber bundle activated, we calculated the maximum activating function, defined as the second spatial derivative of extracellular voltage, along the length of each white matter fiber. All activating function and percent activation calculation and interpolation was completed using MATLAB 2016b.

RESULTS

Fiber-Specific White Matter

We examined fixelwise changes in white matter between pain and control groups using FD, FC, and FDC as metrics. There were no significant differences in FD between groups. There was, however, significantly increased FC ($p < 0.05$ FWE corrected) in a localized region of the splenium of the corpus callosum seen in pain patients when compared to controls. Decreasing the alpha threshold to $p < 0.1$ (FWE corrected), elucidated FC increase in a distinct commissural pathway from the splenium to the major forceps of the corpus callosum that borders the retrosplenial complex, posterior cingulate cortex (PCC), and fusiform. A similar pattern of increased FDC in pain subjects is also evident at this alpha level

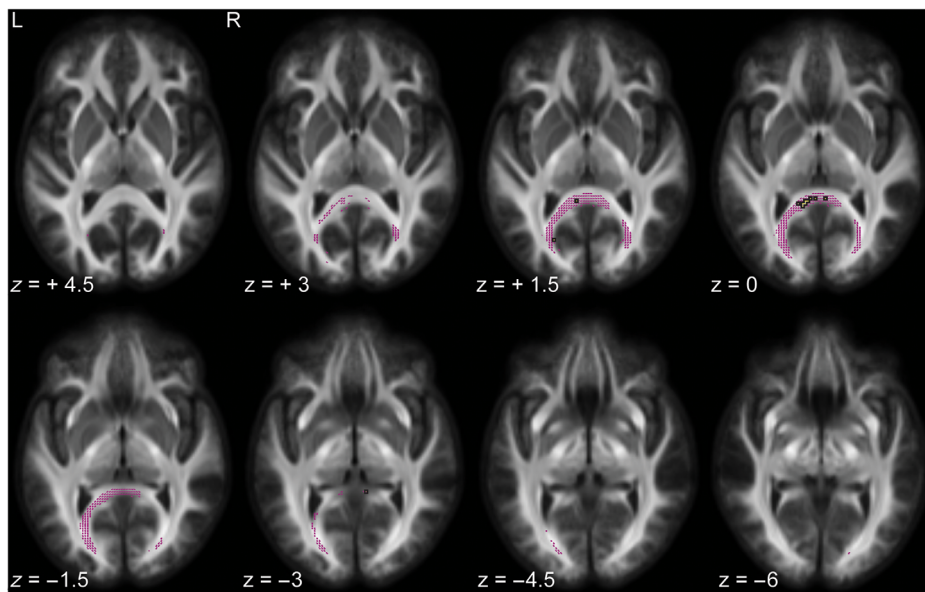


Figure 1. Increased FC in NP subjects compared to controls. Map of fixels showing increased white matter FC in NP subjects compared to control subjects. Significant increases in FC ($p < 0.05$ FWE corrected) were seen in the splenium of the corpus callosum primarily in a small region even with the anterior commissure/posterior commissure (AC/PC) plane. Fixels with significantly increased FC ($p < 0.05$ FWE corrected) are yellow and are outlined in black. The pattern of increased FC extended bilaterally through the corpus callosum, this extended pattern is thresholded at $p < 0.1$ FWE for display purposes and is shown in magenta. Z values are in millimeters and are relative to the AC/PC plane. [Color figure can be viewed at wileyonlinelibrary.com]

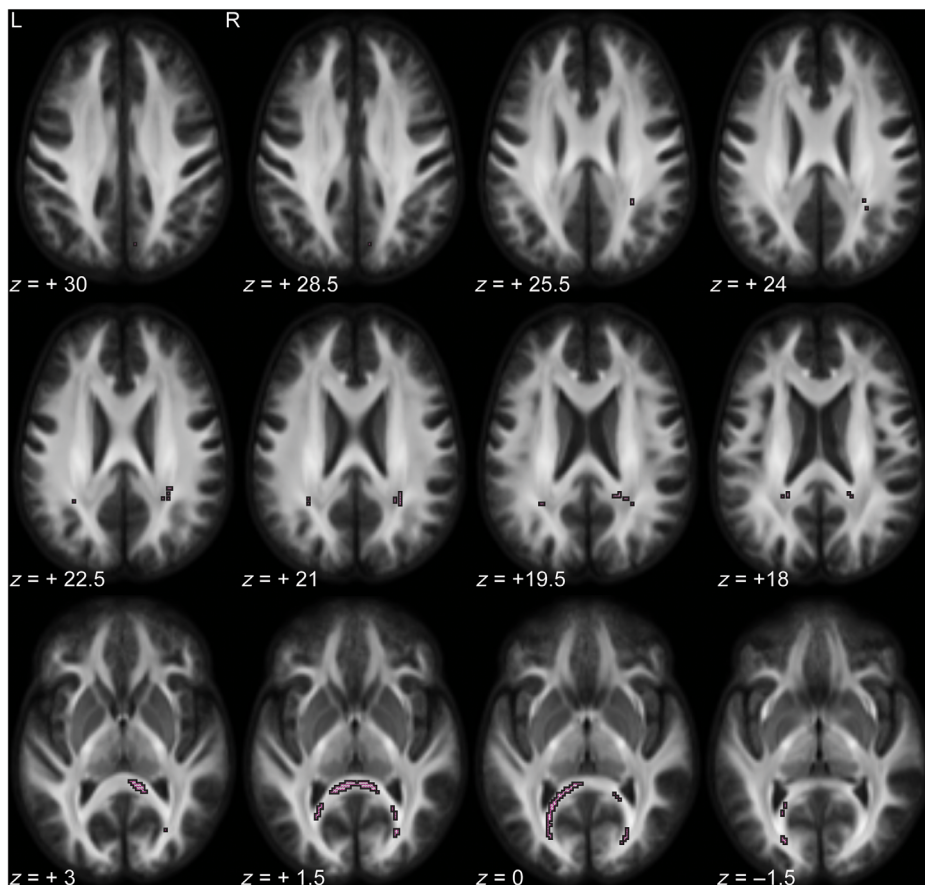


Figure 2. Increased FDC in NP subjects compared to controls. Map of fixels showing increased white matter FDC ($p < 0.1$ FWE corrected) in NP subjects compared to controls. Small clusters of increased FDC were seen in bilaterally in parietal regions. Increased FDC also was seen in the splenium of the corpus callosum in a similar pattern to that seen in groupwise comparisons of white matter FC. Fixels with increased FDC are shown in magenta and outlined in black. Z values are in millimeters and are relative to the AC/PC plane. [Color figure can be viewed at wileyonlinelibrary.com]

($p < 0.1$ FWE corrected) in the corpus callosum. Additionally, FDC was increased bilaterally in small superior parietal areas. Maps of FC and FDC increase in the pain group are shown in Figures 1 and 2, respectively. None of the white matter metrics showed any region of decrease in the pain group compared to controls.

Fiber Bundle Connectivity

By filtering a whole-brain tractogram generated from an FOD template made using this study population, we identified five distinct fiber bundles that pass through fixels with significantly increased FC in pain subjects compared to controls. These five fiber bundles consisted of bilateral superior bundles (Fig. 3a,b) that travel anteriorly through cingulum and the superior longitudinal fasciculus; bilateral inferior bundles (Fig. 3c,d) that converge in the splenium of the corpus callosum, but travel anteriorly in a dispersed pattern through the inferior longitudinal fasciculus; and a posterior bundle (Fig. 3e) that projects posteriorly in both hemispheres.

The left superior bundle (Fig. 3a) showed connectivity primarily between the left hippocampus and regions within ipsilateral prefrontal, orbitofrontal, and cingulate cortices. There were a smaller number of left ipsilateral connections between the cingulate and prefrontal cortices, thalamus and prefrontal cortex, and occipital and prefrontal cortices. The right superior bundle had a substantial proportion of connections between the right cingulate isthmus and regions within ipsilateral prefrontal cortex and PCC. Other connections within the right superior bundle included right ipsilateral connections between the cingulate isthmus and the accumbens, anterior cingulate cortex, and orbitofrontal cortex. There were also commissural connections between left parietal cortex and the right cingulate and prefrontal cortices, and between left occipital and right prefrontal and orbitofrontal cortices. The left inferior bundle primarily showed connections ipsilaterally between left parietal cortex and entorhinal cortex, left parietal cortex and temporal cortex, and left occipital and temporal cortex. There were also a substantial number of contralateral connections between right superior cortex and left temporal cortex. The right inferior bundle connected regions of the left occipital and parietal cortices with right fusiform, temporal cortex, thalamus, caudate, and hippocampus. Finally, the posterior bundle consisted of commissural connections between left and right parietal and occipital cortices. Detailed information on all of the connected nodes within each of the connectomes generated for each bundle can be found in Supplementary Material Table S1.

DBS Activation

We used computational models to predict the percentage of activation for each of the five bundles identified in “Fiber Bundle Connectivity” section for six different DBS target locations (Fig. 4). For each target, the location of the active contact is indicated with a magenta dot on an axial slice view of the study-specific FOD template in the top row of Fig. 4a–f, with the resultant percentage activation of each bundle plotted on the bottom row. A volume rendering of all of the DBS target locations is shown in Fig. 4g–i.

First, we attempted to isolate each fiber bundle. The goal of this was to activate a substantial proportion of a single bundle without spread into any of the other bundles. In the case that stimulation of one or more of our bundles of interest resulted in unwanted side-effects with clinical application, we were

interested in identifying feasible targets that could theoretically stimulate the other bundles individually. We were able to achieve reasonable separability in this regard with the target locations identified to isolate the left and right superior fiber bundles

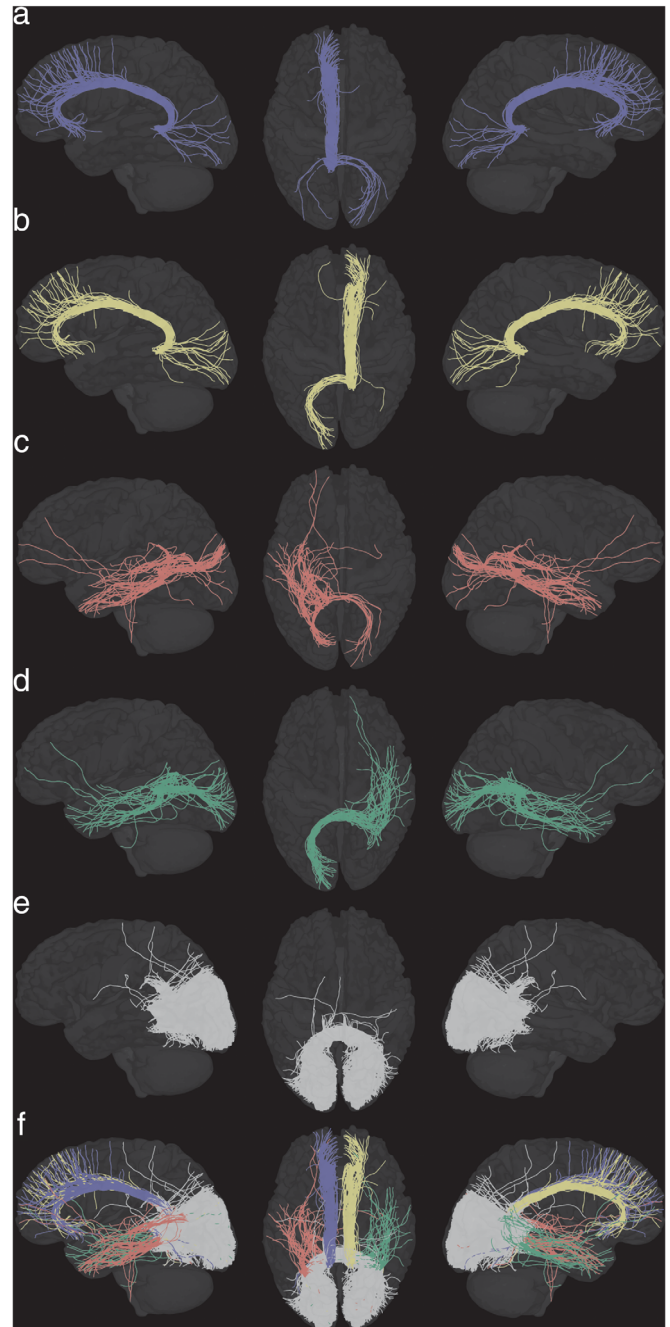


Figure 3. White matter fiber bundles passing through fixels with increased FC in NP subjects compared to controls. Fixels showing significantly increased FC ($p < 0.05$ FWE corrected) in NP subjects compared to controls were used as seeds in order to filter a whole brain tractogram generated from a template FOD map of this study population. The remaining fibers were separated into bundles based upon common endpoints, providing five fiber bundles common to this cohort (shown together in f); left (a) and right (b) superior bundles, traveling through cingulate to prefrontal, orbitofrontal, and subcortical regions; left (c) and right (d) inferior bundles traveling in a more dispersed pattern to temporal, orbitofrontal, and subcortical regions; and a dense commissural bundle (e) traveling between bilateral occipital and inferior parietal regions. [Color figure can be viewed at wileyonlinelibrary.com]

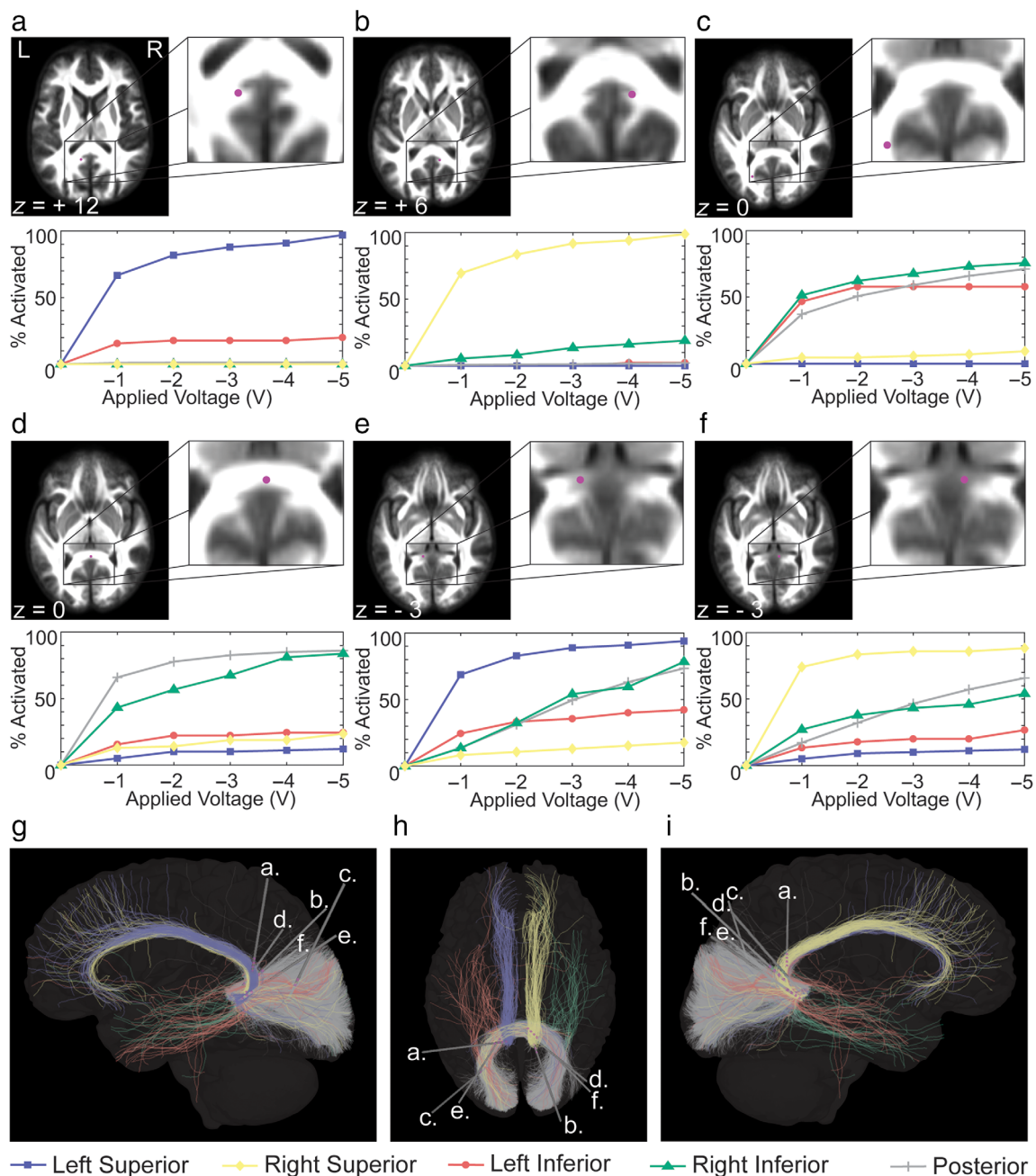


Figure 4. Simulated fiber bundle activation with varied voltage and DBS electrode location. Electrodes were manually placed and FEM-based simulations of DBS were performed in order to identify realistic target locations in which a substantial proportion of each fiber bundle could be activated with bilateral or unilateral implantation. a–f. The location of the active contact is shown (top) along with the predicted total fiber bundle activation for stimulation amplitudes -1 V to -5 V (bottom) using the contact with the maximum activation for each electrode location. In (a–d), DBS electrodes were placed in order to activate each fiber bundle or group—left superior (a), right superior (b), bilateral inferior (c), posterior (d)—individually. In (e, f), DBS electrodes were placed in an attempt to activate a substantial proportion of all of the fiber bundles in either the left (e) or right (f) hemisphere. g–i. Left (g), superior (h), and right (i) views of the final DBS lead trajectories for each of the six electrode locations. L = left; R = right. Z values are in millimeters and are relative to the AC/PC plane. [Color figure can be viewed at wileyonlinelibrary.com]

(shown in Fig. 4a,b, respectively). At the left target location with an applied voltage of -1 V to -5 V, we predicted 67–97% activation of the left superior bundle, 16–20% activation of the left inferior bundle, and less than 1.5% activation of the other three bundles. Similarly, at the right target location we predicted 77–99% activation of the right superior bundle, 8–30% of the right inferior bundle, 1–10% of the posterior bundle, and less than 2.25% of the left superior and inferior bundles.

Both of the inferior bundles and the posterior bundle proved to be inseparable, due to their common pathways through the splenium and diffuse distribution outside this area. We were therefore unable to identify a target location that could substantially activate one of the three bundles in isolation. Instead, we identified a target location at which we could activate both inferior bundles at the same time using a single DBS electrode with minimal activation of either of the superior bundles. At this target

location, we were able to predict 52–76% activation of the right inferior bundle, 47–58% activation of the left inferior bundle, 37–71% of the posterior bundle, 5–9% of the right superior bundle, and no activation of the left superior bundle with -1 V to -5 V stimulation amplitude (Fig. 4c). We then identified a target location in an attempt to activate the greatest proportion of the posterior bundle, again with little activation of either superior bundle. With this target, we predicted 66–86% activation of the posterior bundle, 43–84% of the right inferior bundle, 16–24% of the left inferior bundle, 13–24% of the right superior bundle, and 5–12% of the left superior bundle. These results indicate that although the inferior and posterior bundles were inseparable, they can be stimulated with a reasonable degree of isolation from the superior fiber bundles.

Finally, we identified target locations in an attempt to activate a large proportion of all of the fiber bundles at the same time. There were not any locations in which a majority of all five fiber bundles could be activated with a single DBS lead. We therefore identified unilateral targets that could activate the fiber bundles within each hemisphere. In an attempt to activate the left superior and inferior bundles along with the posterior bundle (Fig. 4e), again with -1 V to -5 V stimulation amplitudes, we predicted 73–96% activation of the left superior bundle, 18–40% of the left inferior bundle, 10–68% of the posterior bundle, 8–65% of the right inferior bundle, and 8–18% of the right superior bundle. On the right side (Fig. 4f), we were able to identify a target location with predicted activations of 74–88% of the right superior bundle, 27–54% of the right inferior bundle, 17–66% of the posterior bundle, 13–27% of the left inferior bundle, and 5–12% of the left superior bundle. These two target locations were determined using the percent activation of each fiber bundle on the left or right hemisphere of the brain along with the posterior bundle (e.g., for the left target location, we looked at the percent activation of the left superior bundle, the left inferior bundle, and the posterior bundle). The two targets identified were those in which the largest proportion of all three bundles together were activated with the range of applied amplitudes that we tested.

DISCUSSION

Fiber-Specific White Matter

In this study, we identified localized regions of significant, fiber-specific white matter FC increase associated with NP after SCI near the midline of the splenium of the corpus callosum. This is a highly connected commissural pathway with fiber tracts projecting to regions responsible for a wide range of visual, emotional, and sensorimotor processes (35,36). Previous work has identified correlations between structural changes near the midline of the splenium and sensorimotor or pain related clinical findings including ataxia, headache, fatigue, hemiparesis, age-related mobility decline, and chronic musculoskeletal pain (37–39).

Prior to this study, correlations between NP after SCI and structural changes in splenium have not been specifically identified. However, alterations in visual areas connected to this region have previously been associated with NP following limb amputation, and are hypothesized to be a compensatory mechanism for altered visuospatial feedback from the missing limb (40). Distortions in visuospatial perception have been also been shown to be associated with SCI patients who have NP (41). The distinction between SCI-related effects and NP-related perceptual changes is not well classified, however, and may be more responsive to SCI completeness than to other factors (42). All of the subjects in this

study had sustained an SCI and there were no differences between groups in the ratio of complete and incomplete injuries. Therefore, it is more likely that the increased FC seen in our pain subjects is reflective of changes more closely related to emotional and sensorimotor processes connected through the splenium than to visuospatial deficits.

White Matter Connectivity

Our tractography results indicate a direct connection between increased FC in the splenium and limbic circuitry, which is involved in emotional control and sensory-emotional integration (43). Both the superior and inferior white matter bundles associated with regions of FC increase closely follow known limbic pathways and a majority of the fiber tracts within each bundle connect with at least one limbic structure directly. Corticolimbic circuitry has been implicated in nociceptive sensitivity (44) and the chronification of pain (10,45). These effects are particularly evident in in prefrontal cortex, hippocampus, and cingulate cortex (10), which were major components of our superior bundles. Changes in white matter in these regions of the brain have been shown to be correlated with increased pain severity, affect, and predisposition to development of chronic symptoms (19–21). In particular, white matter changes in dorsolateral prefrontal cortex (DLPFC) were shown to be directly correlated with increases in perceived pain severity and functional impact (21). Although the role of the DLPFC in pain is not well understood, abnormalities in this area have been shown to reverse with reduction of symptoms (46). Changes in medial prefrontal cortex are, on the other hand, associated with pain chronification (19). Our superior bundles were largely connected to these regions through the cingulate, which is widely known to be involved in perceptual and emotional processing of pain (47). Nociceptive stimuli have also been shown to decrease activity in the ventral PCC, which is involved in self-referential cognition, and was again highly connected in the superior bundles identified in this cohort (47). Further, our previous work in this cohort showed increased white matter and functional connectivity associated with NP in several regions that are directly downstream of fiber-specific neurostructural changes identified here (S.R. Black et al., unpublished data). These clinical associations with the regions of the brain identified in our results suggest that therapeutic intervention targeted to our fiber bundles may be beneficial for treating NP in the SCI cohort.

DBS Targeting for NP After SCI

Neurostructural changes in splenium associated with various pathologies have been shown to reverse with symptom improvement (38,48,49), indicating that the regions of increased white matter FC associated with NP in this study may be responsive to therapeutic intervention. DBS has been successfully used to treat a variety of pain conditions for several decades (50). However, attempts to treat NP with DBS in previously targeted regions has proven to be largely ineffective and the need for the identification of new targets specific to NP populations has been necessitated (51). More recent work has hypothesized that classifying the condition-specific neurological changes within the limbic system due to NP may prove to be particularly important in the identification of such therapeutic targets (10). Our results align well with these hypotheses and we have identified a localized region

specific to the SCI population with NP that may result in the improvement of NP symptoms with DBS treatment.

We have implemented a novel, fiber-based strategy to identify population-specific DBS targets within the limbic system for future study in the effective treatment of NP after SCI. Surgically induced lesions in the splenium have been successfully used for the treatment of medically refractory epilepsy (52), indicating that it is viable as an implantation target and may respond to other forms of therapy. With this small feasibility study, we were able to identify bilateral implantation targets that predicted a substantial majority of activation in four out of five fiber bundles. Although a majority of the left inferior bundle was not activated by the left or right DBS electrode location, the distribution of fibers was such that we expect the combined effects of bilateral implantation would decrease this deficit substantially. The splenium of the corpus callosum highly connected to visual cortex and regions involved in memory and cognitive integration, which may result in unwanted side-effects with the application of DBS to all five fiber bundles. We therefore identified additional targets that could be predicted to activate each of our identified fiber bundles in isolation. Based on these results, we hypothesize that fiber-based targeting for DBS of limbic circuitry via the splenium of the corpus callosum is feasible and future work is warranted to assess its efficacy in the treatment of NP after SCI.

Limitations

Limitations of this study include the modest sample size, which was a subset of a larger SCI sample with strict inclusion and exclusion criteria, which allowed us to identify statistically significant changes in white matter structure in a more highly controlled cohort (for more in-depth discussions on this point, see S.R. Black et al., unpublished data). Additional research with a larger cohort of SCI subjects from multiple sites may be beneficial to confirm the results presented here. Other than the presence or absence of NP, the only significant difference between our subject groups was anxiety and depression severity, which introduces a potential confound. Both anxiety and depression, however, have been shown to be significantly higher in chronic pain populations (53,54). In SCI patients, it was shown that patients' pain contributed significantly to these symptoms and suggested that chronic pain has a cumulative impact on mood symptoms over time (54). This suggests that neuroplastic changes over time may be resultant of NP symptoms as well. We did not have the statistical power to determine if the neurological changes may have been correlated with anxiety and depression symptoms rather than subjects' pain. However, we mitigated this issue somewhat by statistically excluding temporal effects of NP and SCI in our groupwise analysis. We still expect that targeting treatment-based and/or mechanistic research to the neurological regions identified would provide meaningful insight into NP in the SCI cohort.

We also recognize that the cluster of fixels with significant results was small in size. However, the observed pattern of white matter FC increase extended throughout the posterior-inferior corpus callosum for both FC and FDC. Although this larger pattern did not meet the criteria for statistical significance, we estimate that the observed results are consistent with a real difference between pain and control groups for three main reasons. The first is the small sample size used in this study relative to the statistical power for analysis of approximately 500,000 fixels. The second is the clear evidence of an isolated white matter pathway with a conservative increase in alpha

threshold. Finally, this pattern of increased white matter FC and FDC is consistent with our previous results indicating significantly increased white matter connectivity in pain subjects between medial regions of the occipital and parietal cortices (). The fiber tracts associated with increased white matter connectivity largely traveled through the posterior commissural pathway identified in this analysis, further validating that changes in white matter structure in the splenium of the corpus callosum are directly associated with NP in this cohort.

Finally, the accuracy of our simulations was limited by the use of population averaged tractography and the use of the activating function to determine fiber activation. The tractography that we used to generate our fiber bundles only included fibers present within all of our subjects, decreasing the density of fibers within the bundle below physiological norms that would be observed in an individual subject. However, use of the tractogram template also ensured that our fiber bundles would be reproducible in a patient-specific context, which was sufficient for our objective to establish feasibility of DBS stimulation of the bundles. Further, because we were trying to assess the feasibility of a novel therapeutic approach in group atlas space, rather than a patient specific approach, we chose to use the activating function as our model criteria for successful stimulation. We anticipate that future, patient-specific work will incorporate more detailed axon models to better classify voltage distribution in individuals.

CONCLUSIONS

We have identified the splenium of the corpus callosum as a localized region of structural change associated with NP after SCI. White matter fiber pathways that are part of the limbic system and travel directly through this region align with our previous structural and functional neuroimaging studies and these fiber bundles can be feasibly targeted and activated with DBS. Altogether, the known anatomical and functional associations of limbic circuitry with pain and the convergence of our results indicate a need for additional research into this posterior commissural pathway and/or directly connected fiber pathways as potential therapeutic targets to improve neuromodulation treatments for NP after SCI. We have also presented an evidence-based and population-specific approach that may be used as a rationale for the identification of DBS targets for NP in other populations to improve patient outcomes and quality of life.

Acknowledgements

Encrypted patient data storage was provided by the University of Utah Center for High Performance Computing Protected Environment funded by NIH S10 grant 1S10OD021644-01A1. The preprocessing of structural MRI in this study was supported by the Biomedical Imaging and Data Science Core at the University of Utah. Technical support was provided by the Center for Integrative Biomedical Computing at the Scientific Computing and Imaging Institute and was made possible in part by software developed from the NIH P41-GM103545, Center of Integrative Biomedical Computing. Neurosurgical consultation was provided by John D. Rolston, MD, PhD.

Authorship Statement

Shana R. Black carried out study procedures, executed data analysis, and prepared the first manuscript draft; Shana R. Black, Jeffrey Anderson, and Mark Mahan provided intellectual input into the study design, subject recruitment criteria, and methodological approach; Andrew Janson provided intellectual input into the development and implementation of the computational modeling and analysis approach; Christopher R. Butson provided project guidance as well as the computational resources necessary for the completion of the project; and all authors participated in critical review of the manuscript.

How to Cite this Article:

Black S.R., Janson A., Mahan M., Anderson J., Butson C.R. 2021. Identification of Deep Brain Stimulation Targets for Neuropathic Pain After Spinal Cord Injury Using Localized Increases in White Matter Fiber Cross-Section. *Neuromodulation* 2021; E-pub ahead of print. DOI:10.1111/ner.13399

REFERENCES

- Finnerup NB, Haroutounian S, Kamerman P et al. Neuropathic pain: an updated grading system for research and clinical practice. *Pain* 2016;157:1599–1606.
- Center NSCIS. Spinal Cord Injury Facts and Figures at a Glance 2020 SCI Data Sheet. 2020. www.msctc.org/sci/model-system-centers
- Burke D, Fullen BM, Stokes D, Lennon O. Neuropathic pain prevalence following spinal cord injury: a systematic review and meta-analysis. *Eur J Pain* 2017;21:29–44.
- May A. Chronic pain may change the structure of the brain. *Pain* 2008;137:7–15.
- Wiech K. Deconstructing the sensation of pain. *Science* 2016;354:584–587.
- Apkarian AV, Sosa Y, Sonty S et al. Chronic back pain is associated with decreased prefrontal and thalamic gray matter density. *J Neurosci* 2004;24:10410–10415.
- Smallwood RF, Laird AR, Ramage AE et al. Structural brain anomalies and chronic pain: a quantitative meta-analysis of gray matter volume. *J Pain* 2013;14:663–675.
- Schmidt-Wilcke T, Leinisch E, Gänßbauer S et al. Affective components and intensity of pain correlate with structural differences in gray matter in chronic back pain patients. *Pain* 2006;125:89–97.
- Rodríguez-Raecke R, Niemeier A, Ihle K, Ruether W, May A. Brain gray matter decrease in chronic pain is the consequence and not the cause of pain. *J Neurosci* 2009;29:13746–13750.
- Baliki MN, Apkarian AV. Nociception, pain, negative moods, and behavior selection. *Neuron* 2015;87:474–491.
- Maclean PD. The limbic system (“visceral brain”) and emotional behavior. *Arch Neurol Psychiatry* 1955;73:130–134.
- Melzack R, Casey K. Sensory, motivational, and central control determinants of pain. In: Kenshalo D, editor. *The skin senses*. Springfield, IL: CC Thomas, 1968; p. 423–443.
- Alles SRA, Smith PA. Etiology and pharmacology of neuropathic pain. *Pharmacol Rev* 2018;70:315–347.
- Cagnan H, Denison T, McIntyre C, Brown P. Emerging technologies for improved deep brain stimulation. *Nat Biotechnol* 2019;37:1024–1033.
- Honey CM, Tronnier VM, Honey CR. Deep brain stimulation versus motor cortex stimulation for neuropathic pain: a minireview of the literature and proposal for future research. *Comput Struct Biotechnol J* 2016;14:234–237.
- Boccard SGJ, Pereira EAC, Moir L, Aziz TZ, Green AL. Long-term outcomes of deep brain stimulation for neuropathic pain. *Neurosurgery* 2013;72:221–230.
- Prévaire JG, Nguyen JP, Perrouin-Verbe B, Fattal C. Chronic neuropathic pain in spinal cord injury: efficiency of deep brain and motor cortex stimulation therapies for neuropathic pain in spinal cord injury patients. *Ann Phys Rehabil Med* 2009;52:188–193.
- Jermakowicz WJ, Hentall ID, Jagid JR et al. Deep brain stimulation improves the symptoms and sensory signs of persistent central neuropathic pain from spinal cord injury: a case report. *Front Hum Neurosci* 2017;11:177.
- Mansour AR, Baliki MN, Huang L et al. Brain white matter structural properties predict transition to chronic pain. *Pain* 2013;154:2160–2168.
- Huang L, Kutch JJ, Ellingson BM et al. Brain white matter changes associated with urological chronic pelvic pain syndrome: multisite neuroimaging from a MAPP case-control study. *Pain* 2016;157:2782–2791.
- Oosterman JM, van Harten B, Weinstein HC, Scheltens P, Scherder EJA. Pain intensity and pain affect in relation to white matter changes. *Pain* 2006;125:74–81.
- Bouhassira D, Attal N, Fermanian J et al. Development and validation of the neuropathic pain symptom inventory. *Pain* 2004;108:248–257.
- Cleeland CS, Ryan KM. Pain assessment: global use of the brief pain inventory. *Ann Acad Med Singap* 1994;23:129–138.
- Snaith RP. The hospital anxiety and depression scale. *Health Qual Life Outcomes* 2003;1:29.
- Jenkinson M, Beckmann CF, Behrens TEJ, Woolrich MW, Smith SM. FSL. *Neuroimage* 2012;62:782–790.
- Andersson JLR, Sotiropoulos SN. An integrated approach to correction for off-resonance effects and subject movement in diffusion MR imaging. *Neuroimage* 2016;125:1063–1078.
- Andersson JLR, Skare S, Ashburner J. How to correct susceptibility distortions in spin-echo echo-planar images: application to diffusion tensor imaging. *Neuroimage* 2003;20:870–888.
- Smith SM, Jenkinson M, Woolrich MW et al. Advances in functional and structural MR image analysis and implementation as FSL. *Neuroimage* 2004;23: S208–S219.
- Raffelt DA, Tournier JD, Smith RE et al. Investigating white matter fibre density and morphology using fixel-based analysis. *Neuroimage* 2017;144:58–73.
- Raffelt DA, Smith RE, Ridgway GR et al. Connectivity-based fixel enhancement: whole-brain statistical analysis of diffusion MRI measures in the presence of crossing fibres. *Neuroimage* 2015;117:40–55.
- Dhollander T, Raffelt D, Connelly A. Unsupervised 3-tissue response function estimation from single-shell or multi-shell diffusion MR data without a co-registered T1 image. ISMRM Workshop on Breaking the Barriers of Diffusion MRI, Lisbon, Portugal, page 5, 2016.
- Smith RE, Tournier JD, Calamante F, Connelly A. SIFT: spherical-deconvolution informed filtering of tractograms. *Neuroimage* 2013;67:298–312.
- Desikan RS, Ségonne F, Fischl B et al. An automated labeling system for subdividing the human cerebral cortex on MRI scans into gyral based regions of interest. *Neuroimage* 2006;31:968–980.
- Janson AP, Butson CR. Targeting neuronal fiber tracts for deep brain stimulation therapy using interactive, patient-specific models. *J Vis Exp* 2018;2018:57292.
- Aralasmak A, Ulmer JL, Kocak M, Salvan CV, Hillis AE, Yousem DM. Association, commissural, and projection pathways and their functional deficit reported in literature. *J Comput Assist Tomogr* 2006;30:695–715.
- Maddock RJ. The retrosplenial cortex and emotion: new insights from functional neuroimaging of the human brain. *Trends Neurosci* 1999;22:310–316.
- Moscufo N, Wolfson L, Meier D et al. Mobility decline in the elderly relates to lesion accrual in the splenium of the corpus callosum. *Age* 2012;34:405–414.
- Doherty MJ, Jayadev S, Watson NF, Konchada RS, Hallam DK. Clinical implications of splenium magnetic resonance imaging signal changes. *Arch Neurol* 2005;62:433–437.
- Bishop JH, Shpaner M, Kubicki A, Clements S, Watts R, Naylor MR. Structural network differences in chronic musculoskeletal pain: beyond fractional anisotropy. *Neuroimage* 2018;182:441–455.
- Preißler S, Feiler J, Dietrich C, Hofmann GO, Miltner WHR, Weiss T. Gray matter changes following limb amputation with high and low intensities of phantom limb pain. *Cereb Cortex* 2013;23:1038–1048.
- Osinski T, Martínez V, Bensmail D, Bouhassira D. Interplay between body schema, visuospatial perception and pain in patients with spinal cord injury. *Eur J Pain* 2020;24:1400–1410.
- Ionta S, Villiger M, Jutzeler CR, Freund P, Curt A, Gassert R. Spinal cord injury affects the interplay between visual and sensorimotor representations of the body. *Sci Rep* 2016;6:1–12.
- RajMohanan V, Mohandas E. The limbic system. *Indian J Psychiatry* 2007;49:132–139.
- Ulrich-Lai YM, Xie W, Meij JTA, Dolgas CM, Yu L, Herman JP. Limbic and HPA axis function in an animal model of chronic neuropathic pain. *Physiol Behav* 2006;88:67–76.
- Thompson JM, Neugebauer V. Cortico-limbic pain mechanisms. *Neurosci Lett* 2019;702:15–23.
- Seminowicz DA, Moayedi M. The dorsolateral prefrontal cortex in acute and chronic pain. *J Pain* 2017;18:1027–1035.
- Vogt BA. Pain and emotion interactions in subregions of the cingulate gyrus. *Nat Rev Neurosci* 2005;6:533–544.
- Kato Z, Kozawa R, Hashimoto K, Kondo N. Transient lesion in the splenium of the corpus callosum in acute cerebellitis. *J Child Neurol* 2003;18:291–292.
- Lin Y-W, Yu C-Y. Reversible focal splenium lesion—MRS study of a different etiology. *Acta Neurol Taiwan* 2009;18:203–206.
- Bittar RG, Kar-Purkayastha I, Owen SL et al. Deep brain stimulation for pain relief: a meta-analysis. *J Clin Neurosci* 2005;12:515–519.
- Hamani C, Schwab JM, Rezaei AR, Dostrovsky JO, Davis KD, Lozano AM. Deep brain stimulation for chronic neuropathic pain: long-term outcome and the incidence of insertional effect. *Pain* 2006;125:188–196.
- Ho AL, Miller KJ, Cartmell S, Inoyama K, Fisher RS, Halpern CH. Stereotactic laser ablation of the splenium for intractable epilepsy. *Epilepsy Behav Case Rep* 2016;5:23–26.

53. McWilliams LA, Goodwin RD, Cox BJ. Depression and anxiety associated with three pain conditions: results from a nationally representative sample. *Pain* 2004; 111:77–83.
54. Craig A, Tran Y, Siddall P et al. Developing a model of associations between chronic pain, depressive mood, chronic fatigue, and self-efficacy in people with spinal cord injury. *J Pain* 2013;14:911–920.

SUPPORTING INFORMATION

Additional supporting information may be found online in the supporting information tab for this article.